Development of a microfurnace dedicated to in situ scanning electron microscope observation up to 1300 °C. III. In situ high temperature experiments

Jérôme Mendonça, Joseph Lautru, Henri-Pierre Brau, Dorian Nogues, Antoine Candeias, Renaud Podor

Development of a microfurnace dedicated to *in situ* Scanning Electron Microscope observation up to 1300°C - Part III: *in situ* high temperature experiments in the Scanning Electron Microscope.

J. MENDONÇA [1,2], J. LAUTRU [1], H.-P. Brau [1], D. NOGUES [2], A. CANDEIAS [2], R. PODOR [1]*

[1]ICSM, Univ Montpellier, CNRS, CEA, ENSCM, Bagnols-sur-Cèze, France

[2]NewTec Scientific, 2 route de Sommières, 30820 CAVEIRAC

* Corresponding author

e-mail: renaud.podor@cea.fr

Tel: 00 (33) 04.66.33.92.02

Mailing addresses:

Dr Jérôme MENDONÇA

NewTec Scientific

2 route de Sommières

30820 CAVEIRAC

FRANCE

Joseph LAUTRU

Institut de Chimie Séparative de Marcoule

Site de Marcoule, Bâtiment 426

BP 17171

F-30207 Bagnols sur Cèze Cedex

France

Henri-Pierre BRAU

Institut de Chimie Séparative de Marcoule

Site de Marcoule, Bâtiment 426

BP 17171

F-30207 Bagnols sur Cèze Cedex

France

Dorian NOGUES

NewTec Scientific

2 route de Sommières

30820 CAVEIRAC

FRANCE

Antoine CANDEIAS

NewTec Scientific

2 route de Sommières

30820 CAVEIRAC

FRANCE

Renaud PODOR

Institut de Chimie Séparative de Marcoule

Site de Marcoule, Bâtiment 426

BP 17171

F-30207 Bagnols sur Cèze Cedex

France

Abstract: The FurnaSEM microfurnace was installed in the chamber of a scanning electron microscope to carry out *in situ* experiments at high temperature and test its limits. The microfurnace was used in combination with different types of detectors (Everhart-Thornley, for the collection of secondary electrons in a high vacuum; gas secondary electron detector for the specific collection of secondary electrons in the presence of gas; Karmen© detector for the collection of backscattered electrons at high temperature). Experiments carried out on various samples (metal alloys and ceramics) show that the microfurnace operates in both high-vacuum and low-vacuum modes. Temperature ramp rates during temperature cycles applied to the sample range from 1°C/min to 120°C/min (temperature rise) and 1°C/min to 480°C/min (controlled and natural cooling). The maximum temperature at which images were recorded up to 25kX magnification was 1340°C, with a residual air atmosphere of 120Pa. The choice of a flat furnace, with the sample placed directly above it, has enabled innovative experiments to be carried out, such as low-voltage imaging (using a shorter working distance – up to 10 mm - than is possible with conventional furnaces), 3D imaging (by tilting the stage by up to 10°) and high-temperature backscattered electron imaging (using a dedicated detector).

1. Introduction

The main objective in developing the fully metallic high-temperature FurnaSEM microfurnace is to perform high-temperature experiments *in situ* in the SEM chamber. This furnace has been designed to enable versatile work with different atmospheres (reducing, neutral and oxidizing). Typically, commercial and home-developed SEM furnaces are designed for high-vacuum or reducing atmosphere experiments [1,2,3,4,5,6,7]. A few furnaces can work with neutral or oxidizing atmospheres, but existing furnaces are generally unable (for various reasons - sensitivity of the materials used to oxygen, gas release during evacuation, etc.) to cover a wide range of partial pressure of oxygen (i.e. pO_2) [8,9].

The final part of this series of articles will be devoted to testing the FurnaSEM microfurnace under a wide range of operating conditions (high vacuum, residual gas, moderate temperature, high temperature, rapid heating and cooling rates, etc.). The aim is to assess the quality of the images recorded under these conditions, and the suitability of this tool for a wide variety of experimental conditions. Image stability (displacement of the region of interest) will also be assessed as a function of heating or cooling rate, as well as the thermal stability of the furnace (and images) over long periods.

2. Material and methods

In situ high temperature experiments were carried out with both Quanta 200 ESEM FEG (FEI, Eindhoven, The Netherlands) and Quattro S (ThermoFisher Scientific, Eindhoven, The Netherlands) environmental scanning electron microscopes. These two microscopes have similar configurations. They can work at temperature in high vacuum and low vacuum modes (up to 750 Pa). They are equipped with dedicated secondary electron detectors, Everhart-Thornley type for the high vacuum mode and GSED type for the low vacuum mode. The FurnaSEM microfurnace, as described in the previous works [10,11], has been used to heat the samples observed in SEM. Actually, two generations of FurnaSEM device were used.

The first one corresponds to the design optimized and characterized before [10,11]. The device installed in the SEM stage is visible in **Figure 1a**. This device can be equipped to an upper thermal shield in order to maximize the achievable temperature in low vacuum environment (because it is limited to 1200°C with the hot zone not covered as it is demonstrated in Part I). Furthermore, it prevents from overheating the components surrounding the microfurnace in the chamber that undergoes high illumination such as shown in **Figure 1b**.

The second one is the commercial version of FurnaSEM which has been modified to include additional innovations compared to the version used for development tests. It is a larger

microfurnace (77 mm long X 58 mm large X 25 mm height), with a hot zone made completely with platinum. The MgO screw has been removed, and replaced by 3 solid ceramic supports positioned on the sides of the oven's hot zone, guaranteeing temperature homogeneity across the entire surface of the microfurnace (with always a small gap above the position of the thermocouple measuring the sample temperature - see part I). The device installed in the SEM stage is shown in **Figure 1c.** The practical use of the system may come with the mounting of metallic discs to limit the sample thermal drift (see Part II) or a thermal shield to limit radiative heating into the chamber (**Figure 1d**).

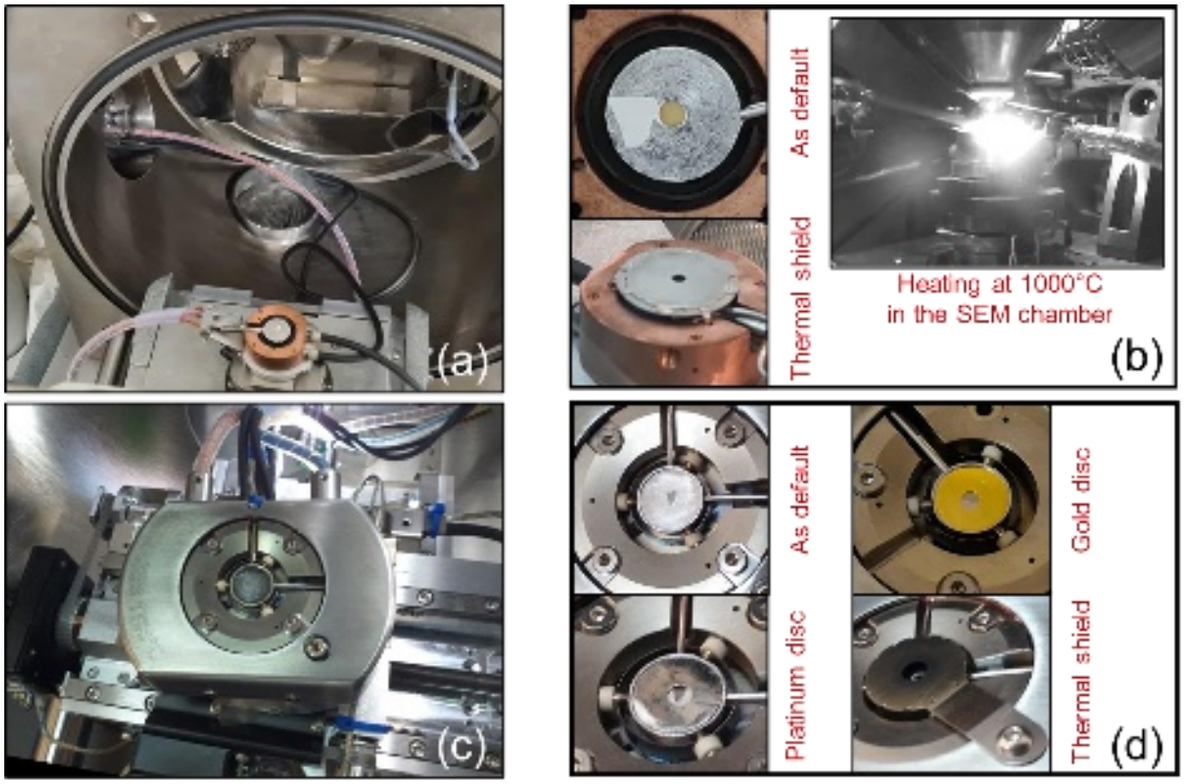

Figure 1 - FurnaSEM microfurnaces used for *in situ* experiments. (a) Original microfurnace [10,11] used for part of the experiments in the Quanta200 FEG ESEM. (b) Zoom in on the hot zone to visualize the sample and heat shield. Image of the high-temperature system in the SEM chamber. (c) Commercial version of the FurnaSEM microfurnace installed on the motorized stage of the Quattro S SEM. (d) Zoom on the hot zone to visualize the samples, thin metal disks and thermal shielding accessories used to limit thermal drift and radiation loss in the chamber.

Few experiments were carried out under a wide range of operating conditions with both FurnaSEM microfurnaces [12,13,14,15]. These experiments demonstrated the flexibility of the microfurnace and its adaptability to a wide range of subjects. Specific experiments to qualify the FurnaSEM microfurnace's potential have also been carried out, and are reported below. The experimental conditions of these experiments are given in **Table 1**.

Table 1 - Experimental conditions relative to the experiments performed for the present study.

Exp name	Sample type	Objective	Isothermal temperature [°C]	Pressure [Pa]	Acceleration voltage [kV]	Frame rate	Experimental details
Phase transformations	Ferrite	Observation of phase transformations from ferrite to austenite and austenite to bainite	900	10^{-4}	15	5s/image up to 900°C; 0.5s/image down to RT	Heating rate = 2°C/s Natural cooling; Movie provided as Multimedia available online
Oxidation of alloys	Ni-base alloy	3D characterization of oxide layers	860	200	18		
Thin films (1)	Ag/CeO_2-Gd_2O_3	Reactivity in thin films	350	120	5		WD = 12mm
Thin films (2)	AgMgSb	Dewetting and reactivity in thin film	572	10^{-3}	20		WD = 12mm
AlSi	AlSi coating in steel	Reactivity and phase formation	600	10	30		Heating rate = 30°C/min WD = 18mm
HT imaging	Al_2O_3	Imaging	1340	100	20		air

3. *In situ* High temperature experiments

3.1. Rapid heating and cooling rates (Phase transformations)

The aim of *in situ* temperature experiments is to reproduce operating conditions in the microscope that correspond to those to which the materials are subjected. Phase transformations in carbon steels are observed during rapid heating and/or cooling ramps. A ferritic steel was heated to 900°C in a high vacuum at a heating rate of 2°C/s, held for one minute in an isothermal stage, then quenched at a natural cooling rate. Images were recorded at 2500X magnification (field of view 50 X 34 µm²) throughout the thermal cycle. Some of the

images extracted from this video are reported in **Figure 2** (Multimedia available online), showing the various transformations taking place during heat treatment. The scientific aspects associated with these transformations are detailed in Seppala *et al* [15]. The raw images recorded (not shown here) indicate that the displacement of the region of interest during heating or cooling is of the order of 20 to 30 µm over the entire temperature range explored. This displacement, even with high temperature variation, is easily corrected manually to keep the region of interest at the center of the images.

Finally, the transformations are observed at the temperatures at which they are expected [15]. This indicates that the device surrounding the sample (gold sandwich foil and heat shield) is sufficiently efficient to guarantee rapid and accurate sample warm-up. The expected sample temperature is 885 (± 15) °C [11]. Furthermore, no sample surface oxidation is observed during this heat treatment, indicating that there is no degassing of the various furnace components in the microscope chamber, as expected.

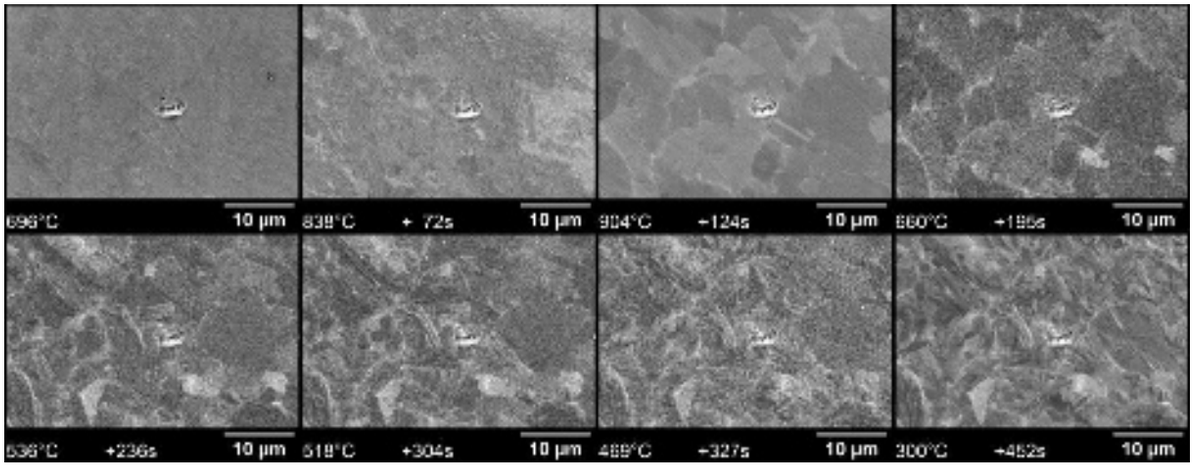

Figure 2 - Series of images showing the ferritic to austenite transformation and austenite to bainite transformation. The times shown on the images correspond to the time difference between the current image and the first image shown. Images were recorded using the SE Everhart-Thornley detector (Multimedia available online).

The actual thermal path followed by the sample is illustrated in **Figure 3**. In terms of temperature rise and isothermal holding, it is perfectly in line with what was expected and in agreement with the measurements reported in parts 1 and 2 of this series of articles [10,11]. The isothermal furnace temperature is 905°C (for a programmed temperature of 900°C). The heating rate is exactly as programmed, i.e. 2°C/s. The furnace (and sample) are cooled naturally by stopping heating at 900°C. As described in Part 1, the cooling rate decreases from 8°C/s at 900°C to 0.2°C/s at room temperature. Finally, the temperature inside the SEM chamber (measured with an additional thermocouple placed in the SEM chamber close to the objective lens – data recorded manually) remains between 17 and 23°C.

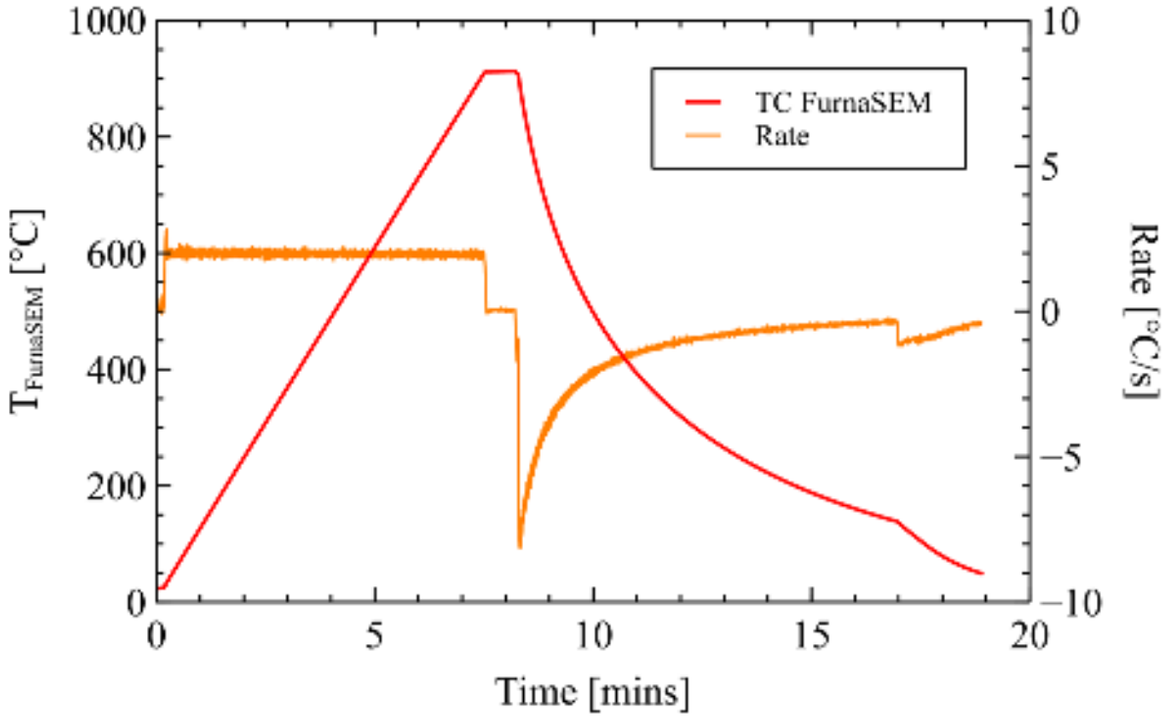

Figure 3 – Heat treatment imposed on the sample. A constant heating rate of 2°C/s is set until reaching a goal temperature of 900°C. Then a high cooling rate ($\sim 8°C/s$) is achieved by using natural cooling. For the entire test, the SEM chamber remains between 17 and 23°C.

3.2. 3D images at high temperature (oxidation of alloys)

The FurnaSEM microfurnace takes up very little space in the SEM chamber, thanks to the flat geometry of the hot zone surface. It allows work to be carried out at short working distances (up to 10 mm), without significant heating of the SEM chamber elements, and it can be tilted with respect to the axis of the primary electron beam. By recording images at three different tilt angles, image processing software (Alicona MEX, Digital Surf) can be used to reconstruct a three-dimensional image of the sample surface. The geometry of the microfurnace developed in this study enables series of tilted images to be recorded, which are then used to reconstruct an associated image showing the three-dimensional morphology of the sample at high temperature. However, it is essential that the sample undergoes no morphological transformation during image recording. For the moment, this imaging mode remains limited to the characterization of slow transformation processes. By automating image recording and changing the position of the stage, faster transformations can be observed.

The images in **Figure 4** show the evolution of the surface of a coarse-grained chromium-forming alloy during oxidation at 680°C after 5 hours of isothermal heating at 680°C under 200Pa of air. These images highlight the differences in thickness of the oxide layers formed, probably depending on the crystallographic orientation of the grains.

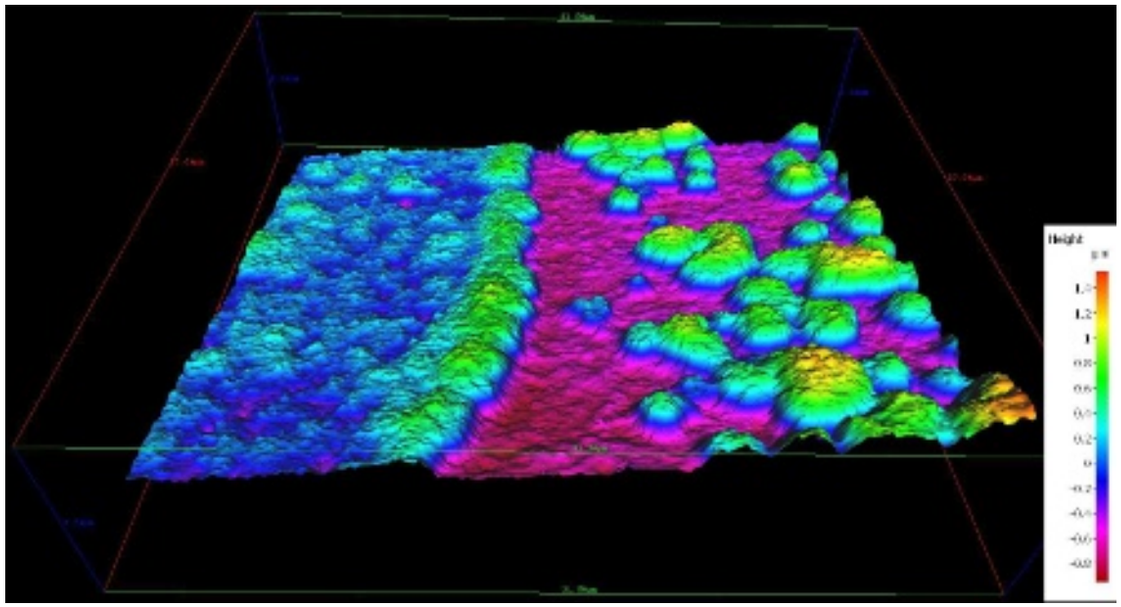

Figure 4 - 3D reconstruction of the surface of a coarse-grained alloy after 5 hours of holding at 680°C under 200 Pa of air.

Series of tilted images can be recorded very quickly (1 to 2 minutes). They can be recorded at different magnifications, opening up new perspectives in the study of material behavior at high temperatures. Such reconstructions were obtained when observing the formation of crystals in glasses of $CsPO_3$ - MoO_3 composition at T = 620°C [16] or when studying the formation of AlSi-type coatings on the surface of steel, between 400 and 900°C [17]. In this study, reconstructions were used to describe the evolution of sample roughness during heat treatment.

3.3. Low voltage imaging (Ag/CeO_2-Gd_2O_3 thin films)

Observation of rearrangement within thin films composed of silver and CeO_2-Gd_2O_3 nanoparticles was carried out at low voltage, in the presence of residual gas (120 Pa of air). Images at 3.5 kV (respectively 5 kV) are shown in **Figure 5**a (respectively **Figure 5**b) at 20,000-fold magnification, for a temperature of 350°C. In preliminary experiments, the microstructure of the sample degraded under the combined effect of temperature and an excessively high acceleration voltage (between 8 and 20 kV). The value of the acceleration voltage was optimized to preserve the integrity of the thin film, and observe its transformation under the single effect of temperature, while attempting to maintain image quality satisfactory for observing fine microstructural details. Experiments were also carried out at 3.5 and 5 kV. Under these imaging conditions, the analyzed zone shows changes identical to those observed on the rest of the sample surface. Despite the temperature and the low acceleration voltage

used, the quality of the images enabled us to discern details of the order of a few tens of nanometers on the sample surface, under 120 Pa of air, using a GSED-type detector to collect the secondary electronic signal.

However, it should be noted that the quality (resolution, i.e. the ability to separate two closely spaced points as two separate entities) of the image recorded at 3.5 kV is lower than that of the image recorded at 5 kV. This can be attributed to a stronger scattering of the primary electron beam in the residual gas thickness to be traversed ("Skirt" effect). Here, this effect has been minimized by working at a reduced working distance (around 12 mm), which is made possible by the flat configuration of the microfurnace's hot zone.

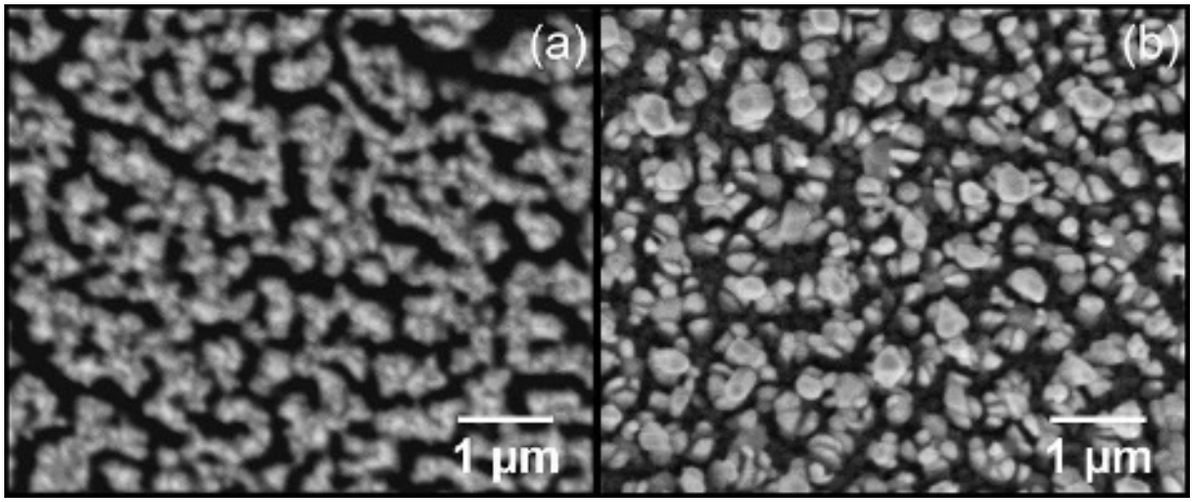

Figure 5 - SE images of thin Ag/CeO_2-Gd_2O_3 films heated *in situ* at 350°C and under gas (120 Pa). (a) Observation at 3.5 kV. (b) Observation at 5 kV.

3.4. High resolution at high temperature (dewetting of MgAsSb thin films)

A MgAsSb compound, deposited as a thin layer on a Si support, was observed up to 572°C under high vacuum, to determine the transformations taking place within this thin layer. The corresponding series of images (**Figure 6**) shows that the thin film dewets and decomposes with increasing temperature. Limited grain growth can also be observed.

The aim of this experiment was to evaluate the ability of microfurnaces to observe nanoscale transformations taking place at high temperature, in high vacuum, on highly oxidizable and brittle materials. No beam effects (accelerated or slowed changes in the observation zone compared with the rest of the sample) were observed. Grain sizes of a few tens of nanometers can be observed. Secondary electrons are collected using an Everhart-Thornley detector. The images obtained under these conditions enable us to assess the

maximum resolution achievable with the furnace when heat-treating complex samples. Here, non-isolated nanoparticles 20-30 nm in diameter can be observed.

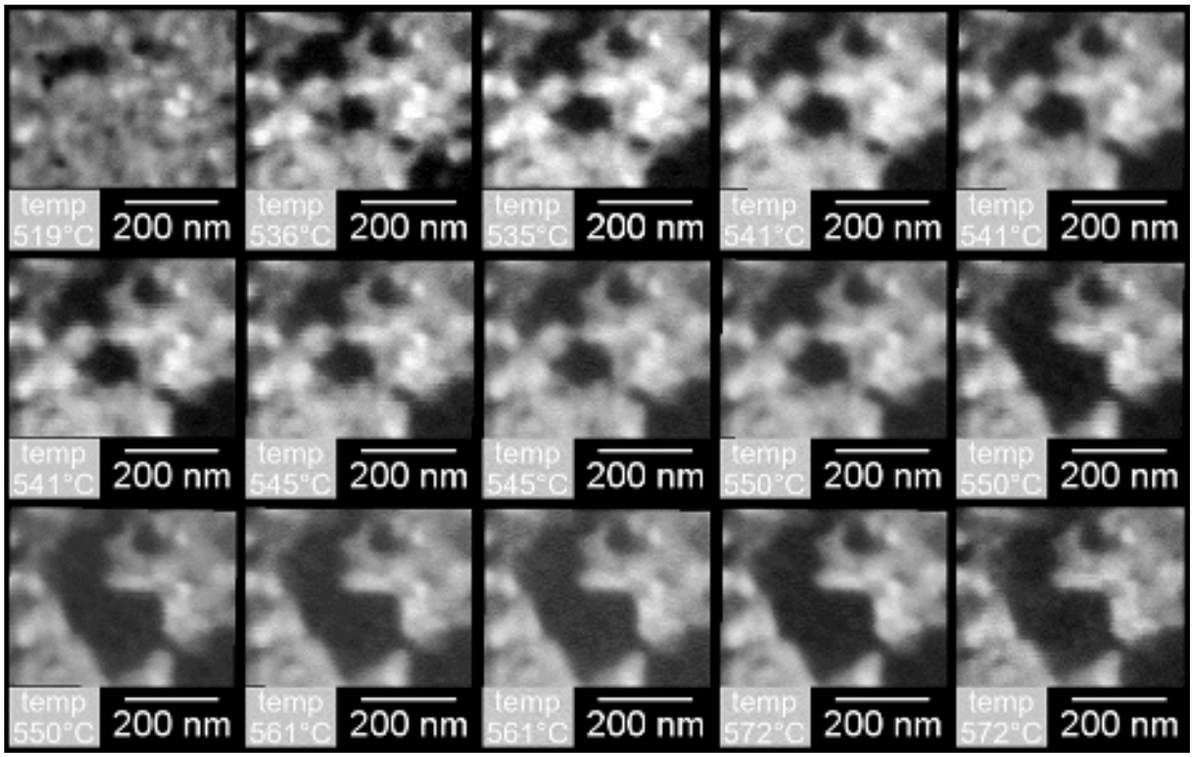

Figure 6 - High magnification series of images recorded on the same area of the surface of a 76 nm thick AgMgSb thin film deposited on a silicon substrate, at different temperatures. 1h35 elapses between the first and last frames of this series. Images are recorded at regular intervals.

3.5. Combination of FurnaSEM with a high temperature BSE detector (AlSi coating)

Collecting backscattered electrons at high temperatures is only possible with a detector capable of withstanding the high heat and illumination induced by thermal radiation from the hot zone of the furnace. Conventional backscattered electron detectors are sensitive to the heat and light of thermal radiation, so cannot be used at high temperatures. The Karmen® detector (Crytur Company™, Czech Republic) has been developed specifically to collect the pure backscattered electron signal at high temperatures. It enables images to be recorded in BSE mode at high temperatures up to 1000°C [13].

By combining the Karmen® detector with the FurnaSEM microfurnace, we were able to record images at 1000°C of an AlSi-type coating deposited on steel undergoing transformation. The BSE images recorded under a graded vacuum of 10 Pa of air, shown in **Figure 7**, demonstrate rapid coating transformations over a narrow temperature range. As the rate of

coating transformation accelerates, the speed of image recording is increased (up to 50 frames per second) to visualize the full range of transformations.

In this configuration, the backscattered electron detector acts as a heat shield. The FurnaSEM microfurnace and Karmen detector can be integrated into any scanning electron microscope, providing a universal technical solution for *in situ* temperature experiments in the presence of gases up to 1000°C.

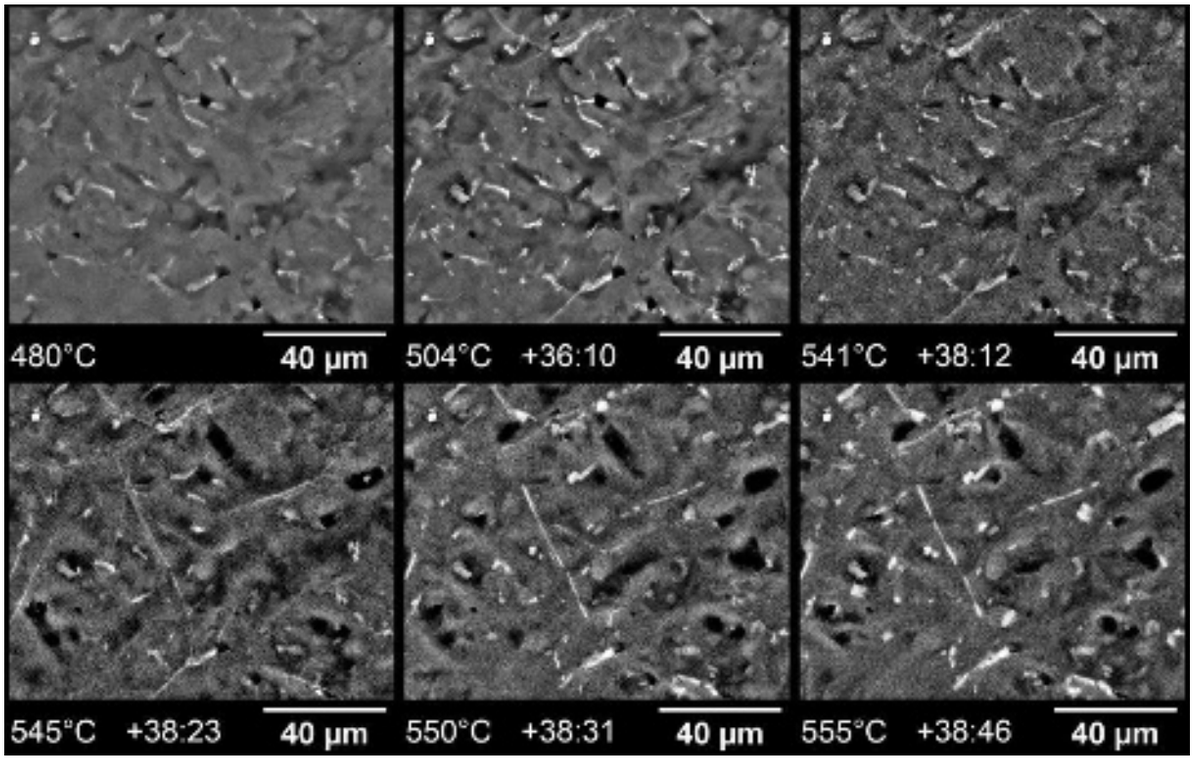

Figure 7 - Micrographs showing the surface microstructural transformations of an AlSi coating deposited on steel between 480 and 555°C, observed under a 10 Pa low vacuum of air and at an acceleration voltage of 30 kV. The times shown on the images correspond to the time difference between the current image and the first image shown.

3.6. High temperature and high-resolution images (Al_2O_3 at 1340°C)

The furnace was heated to a higher temperature than that for which it was designed, i.e. 1340°C, to test its imaging capabilities under extreme conditions. An alumina plate was placed on the hot end, and images were recorded under 100 Pa of air at 20 kV, during the temperature rise and at 1340°C, at different magnifications (**Figure 8**).

The signal-to-noise ratio of images recorded under these conditions is excellent. The quality of the micrographs recorded at the highest magnification makes it possible to distinguish details of around 30 nm on grains a few micrometers in size. It should also be noted

that the settings required to record these images were easy to achieve, and remain stable as the temperature rises. In addition, thermal electron emission remained limited, even at this high temperature (which is in line with the results of Joly-Pottuz *et al*. [18] and linked to the use of a platinum support). These images clearly show that the FurnaSEM microfurnace can work at temperatures up to 1300°C, under gas, while recording images of excellent quality.

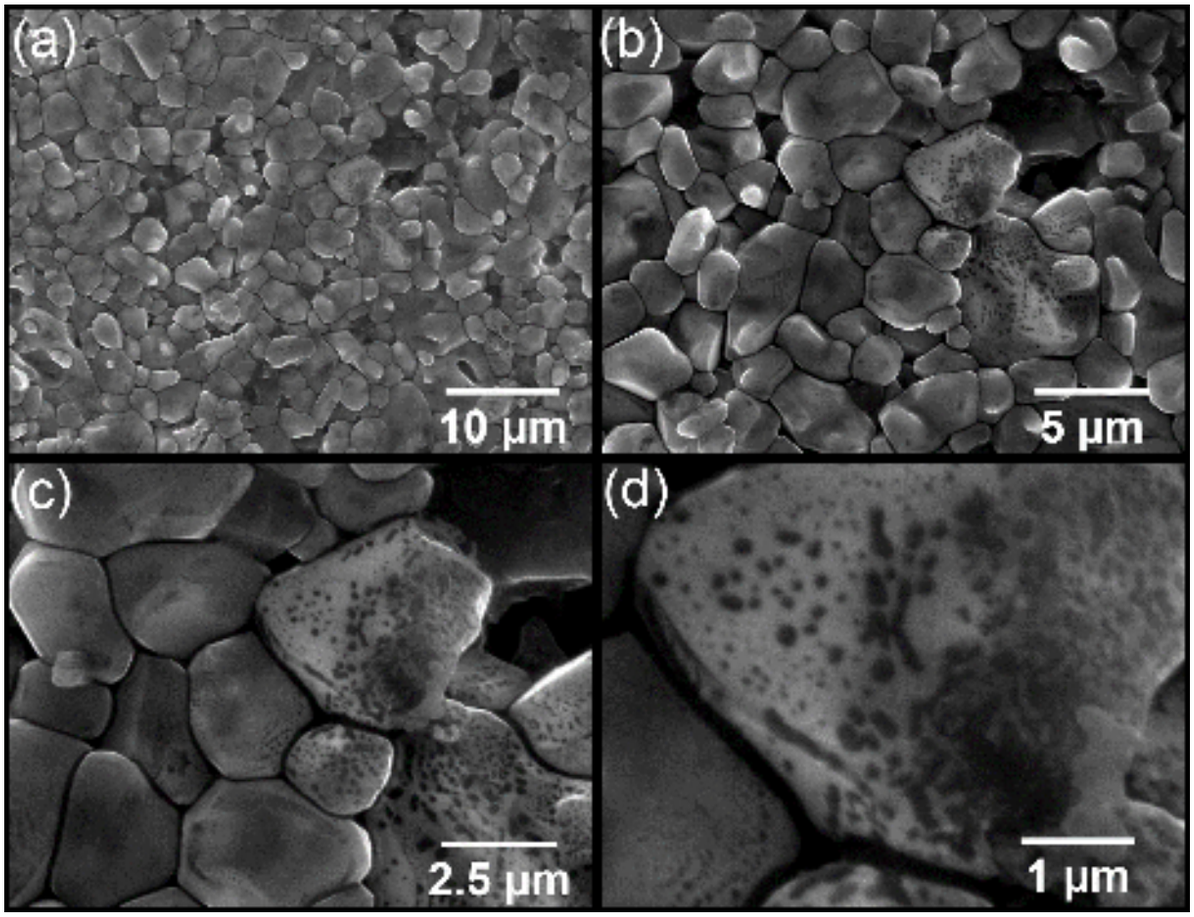

Figure 8 - SEM images of an Al_2O_3 sample heated to 1340°C under 100 Pa of air and at 20 kV. (a) Magnification ×2500, (b) ×5000, (c) ×10,000, (d) ×25,000.

4. Conclusion

Two furnaces were used to carry out these experiments and record these images: the microfurnace used to carry out the qualification tests reported in parts I and II of this series of articles, and a FurnaSEM microfurnace as marketed. The two microfurnaces have similar geometries and technical characteristics. On the commercial microfurnace, the protective hood has been enlarged to allow easy positioning of a removable heat shield.

Optimization of the sample geometry and the way in which a sample is positioned in the furnace (reported in part II) guarantees the temperature homogeneity of the sample. This point was verified by recording phase transformations obtained within the expected temperature

range. Melting point tests were not carried out to avoid damaging the surface of the microfurnace hot zone. Furthermore, the tests carried out did not reveal any increase in temperature in the SEM chamber. The maximum temperature reached with the microfurnace, and for which images were recorded, was 1340°C. This particular point validates the furnace's operation under very high-temperature conditions and its design.

The FurnaSEM microfurnace opens up new opportunities of studies. It has been possible to couple a high-temperature BSE detector with the microfurnace. The main results are reported in another work [13]. This detector operates in high vacuum and degraded vacuum modes, and can be combined with microscopes other than those used in this work. Experiments were carried out under high vacuum, and under degraded vacuum (with oxidizing, neutral or reducing gases), without any particular difficulty. Coupled with the Karmen detector, the FurnaSEM microfurnace makes it possible to carry out experiments in degraded vacuum mode in low-vacuum microscopes not initially designed for *in situ* experiments.

Other imaging modes previously inaccessible at high temperatures can now be implemented, thanks to the short working distance associated with the flat geometry of the furnace's hot zone. Working at low voltages (up to 3.5 kV) has been possible up to 350°C to limit the effect of the electron beam on the sample surface. This temperature is probably not the maximum for which this imaging mode can be used. In addition, 3D reconstructions of a sample surface have been obtained from series of 3 tilted images. Here again, the recording of these images is facilitated by the geometry of the furnace and is very rapid (of the order of one minute). Thus, if the kinetics of the sample surface transformation are slow enough, it may be possible to record a series of 3D images of the sample surface during a long-term experiment. In this case, the evolution of the sample's roughness and/or its volume increase can be studied.

The FurnaSEM microfurnace can also be used to perform *in situ* EBSD experiments at high temperatures up to 1000°C and to observe phase transformations [19]. Taylor *et al*. [20] studied the transformation of austenite into bainite and martensite during sample cooling. Robson *et al.* [21] observed the competition between continuous and discontinuous precipitation in magnesium alloys, treating an alloy of the Mg-Al system at 180°C. In this case, images were recorded *in situ* with a conventional BSE detector and EBSD scans were recorded at room temperature after quenching the sample.

The microfurnace can still be modified to suit user requirements. One of the options being explored is the development of a device for controlling the cooling rate of samples, and in particular the possibility of cooling a sample at up to 20°C/s for rapid quenching. At the same time, computer programs will be developed to control the repositioning (centering of a region of interest) of images and their rapid recording.

All the work carried out and presented in this series of articles demonstrates the experimental possibilities offered by the FurnaSEM microfurnace. The approach, which combines numerical calculations using a digital twin and experimental validation of the data obtained using a real prototype, has led to the construction of a furnace that meets all the initial requirements defined as design criteria. It can be used to carry out *in situ* experiments in the chamber of a SEM covering a wide range of scientific fields. Technical solutions have been tested and validated to overcome one of the major difficulties encountered when using such devices, namely precise control of the sample temperature measurement. Finally, minor adjustments were made to the initial prototype to produce a microfurnace that is now operational and reliable.

ACKNOWLEDGMENT

The authors want to thank Pr Michel Vilasi and Pauline Vilasi (Université de Lorraine), Aarne Pohjonen and Vahid Javaheri (University of Oulu), Alain Portavoce (Aix-Marseille University), Mathias Barreau (University of Caen Normandy) for providing samples.
The authors would like to thank the following organisations for helping to fund all or part of this work: the Région Occitanie and FEDER (Readynov Project Call) have funded the FurnaSEM project (2018-2021). Jerome Mendonça's PhD thesis (2019-2022) was funded by the Association Nationale de la Recherche et de la Technologie (ANRT) through the Cifre program.

AUTHOR DECLARATIONS

Conflict of Interest

The authors have no conflicts to disclose.

Author Contributions

Jérôme. Mendonça : Writing – original draft (lead); Data curation (lead); Methodology (equal); Investigation (equal).

Joseph Lautru: Investigation (equal); Methodology (equal).

Henri-Pierre Brau : Data curation (supporting) ; Methodology (equal); Investigation (equal).

Dorian. Nogues : Data curation (supporting); Investigation (supporting).

Antoine Candeias: Funding acquisition (equal lead); Conceptualization (Equal).

Renaud. Podor: Funding acquisition (equal lead); Conceptualization (Equal); Data curation (supporting); Investigation (supporting); Writing – review & editing (lead).

DATA AVAILABILITY

The data presented in this manuscript is available from the corresponding author upon reasonable request.

5. References

[1] R. M. Fulrath, High temperature scanning electron microscopy, in High Temperature Scanning Electron Microscopy , University of California Press, (1972) 347-351. (https://doi.org/10.1525/9780520323230-020)

[2] A. M. Brown, M. P. Hill, A hot stage SEM for gas-solid reaction studies. J. Microscopy (1989) 153[1] 51-62 (DOI:10.1111/j.1365-2818.1989.tb01466.x)

[3] E. Charyshin, N. N. Kinaev, M. Waterworth, D. R. Cousens, N. Calos, T. Bostrom, A. Ilyushechin, In-situ electron microscopy studies of hot filament chemical vapour deposition diamond thin film growth in an Environmental SEM. phys. stat. sol. (a) (1996) 154 43-54 (https://doi.org/10.1002/pssa.2211540106)

[4] M. Nakamura, T. Isshiki, M. Tamai, et K. Nishio, Development of a new heating stage equipped thermal electron filter for scanning electron microscopy (2002) Proceeding of the 15th International Congress on Electron Microscopy Durban, South Africa. p. 17. (Corpus ID: 201694495)

[5] N. Bozzolo, S. Jacomet, R.E. Logé, Fast in-situ annealing stage coupled with EBSD: A suitable tool to observe quick recrystallization mechanisms. Mater. Charac. (2012) 70 28-32 (https://doi.org/10.1016/j.matchar.2012.04.020)

[6] Z.-J. Wang, G. Weinberg, Q. Zhang, T. Lunkenbein, A. Klein-Hoffmann, M. Kurnatowska, M. Plodinec, Q. Li, L. Chi, R. Schloegl, M.-G. Willinger, Direct Observation of Graphene Growth and Associated Copper Substrate Dynamics by in Situ Scanning Electron Microscopy. ACS Nano (2015) 9[2] 1506-1519 (https://doi.org/10.1021/nn5059826)

[7] R. Heard, J. E. Huber, C. Siviour, G. Edwards, E. Williamson-Brown, An investigation into experimental in situ scanning electron microscope (SEM) imaging at high temperature. Rev. Sci. Instrum. (2020) 91 063702 (doi:10.1063/1.5144981)

[8] A. Mège-Revil, P. Steyer, G. Thollet, R. Chiriac, C. Sigala, J.C. Sanchéz-Lopéz, C. Esnouf, Thermogravimetric and in situ SEM characterisation of the oxidation phenomena of protective

nanocomposite nitride films deposited on steel. Surface & Coatings Technology 204 (2009) 893-901 (doi:10.1016/j.surfcoat.2009.06.040

[9] M. Weiser, A. Reichmann, M. Albu, S. Virtanen, P. Poelt, In Situ Investigation of the Oxidation of Cobalt-Base Superalloys in the Environmental Scanning Electron Microscope. Adv. Eng. Mater. (2015) 17[8] 1158-1167 (https://doi.org/10.1002/adem.201500146)

[10] J. Mendonça, H.P. Brau, D. Nogues, A. Candeias, R. Podor, Development of a microfurnace dedicated to *in situ* SEM observation up to 1300°C - Part I: Concept, fabrication and validation. (Submitted)

[11] J. Mendonça, H.P. Brau, D. Nogues, A. Candeias, R. Podor, Development of a microfurnace dedicated to *in situ* SEM observation up to 1300°C - Part II: Study of the thermal response of samples (Submitted)

[12] V. Trillaud, R. Podor, S. Gossé, A. Mesbah, N. Dacheux, N. Clavier, Early stages of UO_{2+x} Sintering by in situ High-Temperature Environmental Scanning Electron Microscopy. Journal of the European Ceramic Society (2020) 40[15] 5891-5899 (https://doi.org/10.1016/j.jeurceramsoc.2020.07.031)

[13] R. Podor, J. Mendonça, J. Lautru, H.P. Brau, D. Nogues, A. Candeias, P. Horodysky, A. Kolouch, M. Barreau, X. Carrier, N. Ramenatte, S. Mathieu, M. Vilasi, Evaluation and application of a new scintillator-based heat-resistant back-scattered electron detector during heat treatment in the scanning electron microscope. Journal of Microscopy (2021) 282[1] 45-59 (https://doi.org/10.1111/jmi.12979)

[14] T. Alatarvas, R. Podor, H. Singh, E.-P. Heikkinen, Q. Shu, In situ Non-metallic Inclusion Observation with High Temperature Environmental Scanning Electron Microscopy. Materials & Design (2023) 232, 112139 (https://doi.org/10.1016/j.matdes.2023.112139)

[15] O. Seppälä, A. Pohjonen, J. Mendonça, V. Javaheri, R. Podor, H. Singh, J. Larkiola, In-situ SEM characterization and numerical modelling of bainite formation and impingement of a medium-carbon, low-alloy steel. Materials & Design (2023) 230, 111956 (https://doi.org/10.1016/j.matdes.2023.111956)

[16] K. Bodiang, L. Delevoye, R. Podor, F. O. Méar, Structural and properties influence of Molybdenum in A_2O-P_2O_5-MoO_3 (A = Na, Ag, Rb, Cs) glasses. Journal of Non Crystalline Solids (2023) 606 122190 (https://doi.org/10.1016/j.jnoncrysol.2023.122193)

[17] R. Podor, X. Le Goff, J. Lautru, H.P. Brau, M. Barreau, X. Carrier, J. Mendonça, D. Nogues, A. Candeias, Direct observation of the topographic changes occurring in materials during heat treatment at high temperature. Microscopy and Microanalysis (2020) 26[3] 397-402 (https://doi.org/10.1017/S1431927620001348)

[18] L. Joly-Pottuz, A. Bogner, A. Lasalle, A. Malchere, G. Thollet, S. Deville, Improvements for imaging ceramics sintering in situ in ESEM. J. Microscopy (2011) 244: 93-100. (https://doi.org/10.1111/j.1365-2818.2011.03512.x)

[19] H. Mansour, S. Burgess, P. Trimby, K. Larsen, J. Donoghue, J. Xu, A. Smith, High-temperature EDS and EBSD Analysis – Enabling In Situ Heating for Direct Observation of Phase Transformations in the SEM. Microscopy and Microanalysis (2023) 29[1] 2085-2086 (https://doi.org/10.1093/micmic/ozad067.1079)

[20] M. Taylor, A. D. Smith, J. M. Donoghue, T. L. Burnett, E. J. Pickering, In-situ heating-stage EBSD validation of algorithms for prior-austenite grain reconstruction in steel. Scripta Materialia 242 (2024) 115924 (https://doi.org/10.1016/j.scriptamat.2023.115924)

[21] J.D. Robson, A.D. Smith, J. Guo, J.M. Donoghue, A.E. Davis, Grain-scale in-situ study of discontinuous precipitation in Mg–Al. Acta Materialia (2024) 263 119497 (https://doi.org/10.1016/j.actamat.2023.119497)